

# Precipitation Hardening A286 Superalloy with Additional 0.8%wt Aluminium for Waste Incinerator Application

Selly Septianissa<sup>1</sup>; Martoni<sup>2</sup>; Ayu Zahra Chandrasari<sup>3</sup>

<sup>1,2,3</sup> Department of Mechanical Engineering, Faculty of Engineering, Widyatama University, Bandung 40125, Indonesia

Publication Date: 2025/03/20

**Abstract:** This study examined how gamma prime and precipitation hardening impact the iron-nickel-based A286 superalloy during a four-hour aging heat treatment at 850°C. The characterization of samples after ageing was done employing a scanning electron microscope (SEM-EDX) to describe the grain structure arrangement, texture, and presentation of gamma ( $\gamma$ ) and gamma prime ( $\gamma'$ ). With an extra 0.8%wt, the data indicated that the main precipitates at temperatures below 840°C were gamma prime. The results demonstrated that the aluminum concentration of the austenitic matrix decreases at 840°C because of the precipitation mechanism involving the  $\gamma$  and  $\gamma'$  phases, which enhances the repassivation capabilities. The Eta phase enlarges at the cost of the gamma prime phase, and the arrangement of  $\gamma'$  precipitates within the matrix might lead to interruptions in the passive layer.

**Keywords:** Superalloy, Precipitation, A286, SEM, Metals and Alloys.

**How to Cite:** Selly Septianissa; Martoni; Ayu Zahra Chandrasari (2025) Precipitation Hardening A286 Superalloy with Additional 0.8%wt Aluminium for Waste Incinerator Application. *International Journal of Innovative Science and Research Technology*, 10(3), 409-413. <https://doi.org/10.38124/ijisrt/25mar399>

## I. INTRODUCTION

The A286 superalloy, a prominent member of the austenitic stainless steel family, is recognized for its exceptional precipitation-hardening capabilities [1], [2]. It is widely utilized in various high-performance applications, particularly within the aerospace industry, due to its excellent combination of strength, corrosion resistance, and cost-effective manufacturability [3], [4], [5]. One of the defining features of the A286 superalloy is the spherical arrangement of face-centered cubic (fcc)  $\gamma'$  Ni<sub>3</sub>(Al,Ti) precipitates, which contribute significantly to its mechanical properties by impeding dislocation motion at elevated temperatures [6], [7], [8]. The  $\gamma'$  phase, though metastable at high temperatures, transforms into the stable hcp eta ( $\eta$ ) Ni<sub>3</sub>Ti phase over extended aging periods [9], [10]. This transformation can alter the alloy's microstructure and consequently affect its mechanical performance [11].

The  $\gamma'$  precipitates play a pivotal role in enhancing the mechanical properties of the A286 superalloy. They act as obstacles to dislocations, thereby strengthening the material, particularly at elevated temperatures. This leads to an increase in both yield and ultimate tensile strength [12], [13]. However, while there has been extensive research on the precipitation strengthening mechanisms, less attention has been paid to investigating how these phases influence the alloy's corrosion resistance, particularly in aggressive

environments such as those encountered in waste incinerators [14], [15], [16]. Given the importance of corrosion resistance in such applications, it is crucial to understand how the microstructural features, including the presence and distribution of  $\gamma'$  and  $\eta$  phases, affect the alloy's performance under high-temperature and corrosive conditions [17], [18].

Despite its exceptional properties, the stability of A286 superalloy can be compromised during aging treatments at temperatures exceeding 730°C. At this temperature, the metastable  $\gamma'$  phase dissolves, leading to the formation of the stable  $\eta$  phase, which results in a deterioration of the material's mechanical properties. This phenomenon has been observed in previous studies and underscores the need to carefully control the aging treatment to preserve the alloy's desirable characteristics [19], [20], [21]. Research has also demonstrated that the composition, size, and distribution of the precipitates can be tailored through heat treatment to meet specific performance requirements [22]. Therefore, understanding the intricate interplay between the alloy's composition, aging treatment, and precipitate behavior is essential for optimizing its performance in demanding applications.

The incorporation of aluminum (Al) into the  $\gamma$  matrix has a notable influence on the precipitation of  $\gamma'$  and  $\eta$  phases. Increasing the aluminum content results in a higher volume fraction of  $\gamma'$  precipitates, which strengthens the alloy and enhances its high-temperature performance [23], [24], [25]. Previous studies have investigated the effects of Al content on the microstructure and mechanical properties of the alloy, particularly focusing on shear strength and microhardness. However, there remains a gap in research regarding the impact of aluminum content on the pitting corrosion resistance and the long-term stability of the alloy, especially in environments where the material is subjected to high temperatures and corrosive conditions [26]. Furthermore, while the influence of other alloying elements like titanium (Ti) on precipitation hardening has been well-documented, the combined effect of Al and Ti on the mechanical and corrosion properties of A286 superalloy has not been comprehensively studied [27], [28], [29].

This study aims to address this gap by investigating the impact of adding 0.8 wt% aluminum to A286 superalloy and its effect on the alloy's microstructure, mechanical properties, and corrosion resistance under aging conditions. By employing a four-hour aging heat treatment at 850°C, the study will examine the behavior of  $\gamma'$  precipitates and their transformation into the  $\eta$  phase, focusing on the resulting changes in the alloy's grain structure, texture, and corrosion resistance. Scanning electron microscopy (SEM) and energy-dispersive X-ray spectroscopy (EDX) will be utilized to analyze the distribution and morphology of the precipitates and to correlate these features with the alloy's performance. Additionally, this research will explore how the aluminum content influences the formation of passive layers and the overall corrosion resistance of A286 superalloy, particularly in the context of waste incinerator applications.

The results of this study will provide valuable insights into the role of aluminum in enhancing the mechanical properties and corrosion resistance of A286 superalloy. By understanding how the concentration of aluminum affects the precipitation behavior and phase stability, it may be possible to optimize the composition and heat treatment processes for specific applications, such as in waste incinerators, where the alloy is exposed to both high temperatures and corrosive environments. Ultimately, the findings of this research could contribute to the development of more durable and cost-effective materials for high-performance applications in extreme conditions.

## II. EXPERIMENTAL PROCEDURES

A Ferro Nickel-based superalloy serves as the substrate in this investigation, Table 1. provides a thorough breakdown of its chemical composition. Employing a Direct Current Electric Arc Furnace (DC-EAF), the alloys were cast to achieve the desired  $\gamma'$ -Ni<sub>3</sub>Al phase, a process lasting 45 minutes. Following casting, a homogenization step was carried out in horizontal furnaces under inert conditions, maintaining a temperature of 1150 °C for 5 hours. Subsequently, all specimens underwent a solutionizing treatment at a temperature of 980°C for one hour, then swiftly

quenched in water. To attain the targeted microstructure, the specimens were subsequently aged isothermally at 840 °C for a duration of 4 hours.

In addition to these processing steps, it is crucial to examine the  $\gamma$  phase's morphology that results from heat treatment, with particular attention given to the incorporation of 0.8 wt% Al. This investigation aims to provide a comprehensive understanding of the impact of aluminum on the mechanical characteristics of superalloys based on iron and nickel across a range of temperatures, enhancing our knowledge of their suitability for various applications.

Table 1. Weight Percentage Chemical Composition (wt.%) of the Fe-Ni based Superalloy.

Alloy	Fe	Ni	Al	Cr	Ti	Mo
Fe-Ni alloy	Balance	26	0.8	15	2	0.25

## III. RESULTS AND DISCUSSION

The analysis conducted using X-ray Diffraction (XRD) findings on the substrate after the deposition showing the  $\gamma'$  phase after four hours of aging at 840°C enhance its mechanical strength for application purposes, as illustrated in Fig 1.

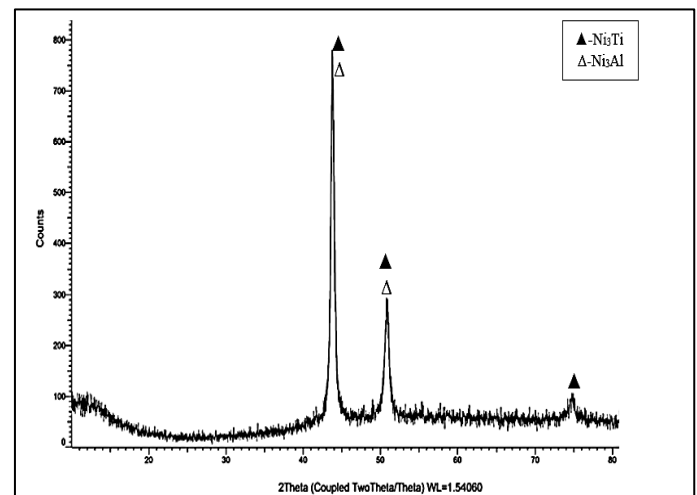


Fig 1. Fe-26Ni-0.8Al-15Cr-2Ti-0.25Mo alloy: XRD Analysis after ageing at 840°C for 4 hours.

The microstructure of the Fe-26Ni-0.8Al-15Cr-2Ti-0.25Mo alloy shown in Fig 2. is the result of SEM analysis, depicting the alloy's microstructure following homogenization and ageing processes at 840°C for 4 hours. The corresponding EDS results are presented in Fig 2. In this image, the morphology of the alloy's  $\gamma'$  precipitates is evident, indicating their potential to provide high strength. The sizes and average distribution of the precipitates are detailed in Table 2.

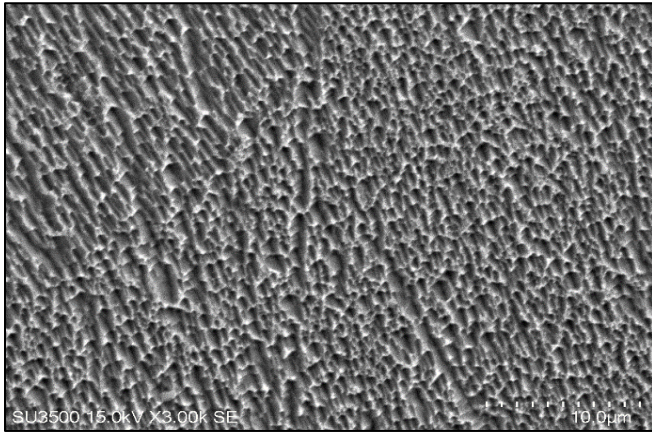


Fig 2. SEM Image of the Substrate Following Heat Treatment

Table 2. Average Size of Precipitates

No.	Precipitate Size (nm)
1	83,87
2	61,503
3	67,708
4	74,365
5	74,376
6	55,423
7	67,725

The SEM analysis reveals the microstructural evolution of the Fe-26Ni-0.8Al-15Cr-2Ti-0.25Mo alloy after undergoing homogenization and ageing treatments at 840°C for 4 hours. The presence of well-defined  $\gamma'$  precipitates signifies the effectiveness of how the heat treatment process enhances the mechanical properties of the alloy. Additionally, the EDS analysis confirms the chemical composition of the precipitates, further validating their role in strengthening the alloy. The data presented in Table 2. offer quantitative insights into the size distribution of the precipitates, which is essential for understanding the alloy's mechanical behavior.

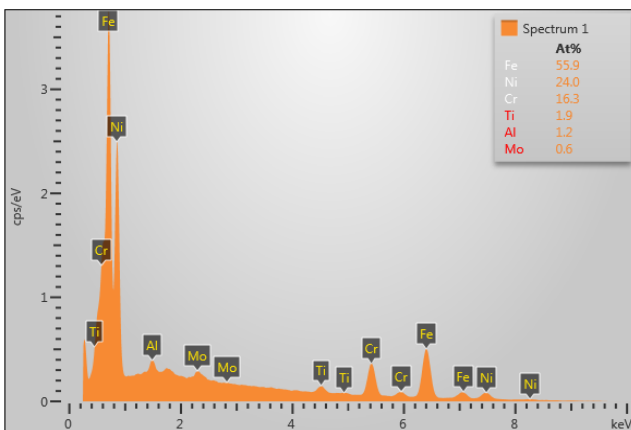


Fig 3. Results of the EDS Tests Plotted Across the Substrate's Whole Surface.

The comprehensive SEM and EDS analyses presented in Figs 2 and 3. along with the accompanying quantitative data in Table 2, provide valuable insights into the microstructural characteristics and composition of the Fe-26Ni-0.8Al-15Cr-2Ti-0.25Mo alloy. These findings aid in the comprehension of the alloy's performance and suitability for various applications requiring high mechanical strength [30], [31].

The calculation of phase percentages in this study was conducted to compare the regions situated amidst the  $\gamma$  and  $\gamma'$  phases within samples subjected to heat treatment in the Fe-26Ni-0.8Al-15Cr-2Ti-0.25Mo alloy. This phase percentage calculation utilized Optimas software. The Table 3 below presents the comparative information regarding the volume fractions of the Fe-26Ni-0.8Al-15Cr-2Ti-0.25Mo alloy [32], [33].

Table 3. Comparing the Fe-26Ni-0.8Al-15Cr-2Ti-0.25Mo Alloy's Volume Fractions.

Phase	Volume Fraction
Gamma	12,04
Gamma prime	87,96

The evident enhancement in performance resulting from the addition of 0.8 wt% Aluminium to the Fe-26Ni-0.8Al-15Cr-2Ti-0.25Mo alloy is noteworthy. The phase percentage calculation provides a clear indication pertaining to the arrangement and ratio of the  $\gamma$  and  $\gamma'$  phases following the heat treatment . This analysis plays a crucial role in comprehending the microstructural changes in the alloy and how they affect mechanical characteristics. The data presented in Table 3 offer compelling evidence supporting the effectiveness of the alloy composition and heat treatment process, which are essential for optimizing its performance in practical applications.

#### IV. CONCLUSIONS

The evident structure of  $\gamma'$  precipitates within the alloy suggests their potential to significantly enhance strength. SEM analysis illustrates the microstructural evolution of the Fe-26Ni-0.8Al-15Cr-2Ti-0.25Mo alloy post-homogenization and ageing, revealing well-defined  $\gamma'$  precipitates indicative of improved mechanical properties due to effective heat treatment. Additionally, EDS analysis confirms the precipitates' chemical composition, further validating their role in alloy strengthening. The quantitative insights from Table 2 are crucial for understanding mechanical behavior, complemented by comprehensive SEM and EDS analyses presented in Figs 2 and 3, along with accompanying quantitative data. Notably, the addition of 0.8 wt% Aluminium demonstrates a significant performance enhancement, particularly evident in the calculated gamma prime percentage of 87.96%, indicating optimized phase distribution post-heat treatment. These findings collectively underscore the alloy's suitability for high-strength applications, highlighting the efficacy of its composition and heat treatment process for practical implementation.

## ACKNOWLEDGMENT

The authors extend their heartfelt appreciation to the Department of Metallurgical Engineering in the Faculty of Mining and Petroleum Engineering at Institut Teknologi Bandung (ITB) and the Department of Mechanical Engineering at Widayatama University for their unwavering support and generous funding. Gratitude is also expressed to the specialists at the National Research and Innovation Agency's Research Center for Advanced Materials, for their valuable contributions. The collaboration and support from all research aides at the ITB Metal Sustainability and Corrosion Laboratory are highly regarded. Funding for this project was offered by the National Research and Innovation Agency.

## REFERENCES

- [1]. P. De Tiedra, Ó. Martín, and M. San-Juan, "Potentiodynamic study of the influence of gamma prime and eta phases on pitting corrosion of A286 superalloy," *J Alloys Compd*, vol. 673, pp. 231–236, Jul. 2016, doi: 10.1016/j.jallcom.2016.02.261.
- [2]. P. De Tiedra, Ó. Martín, and M. San-Juan, "Potentiodynamic study of the influence of gamma prime and eta phases on pitting corrosion of A286 superalloy," *J Alloys Compd*, vol. 673, pp. 231–236, Jul. 2016, doi: 10.1016/j.jallcom.2016.02.261.
- [3]. J. Yang, Z. Zhu, S. Han, Y. Gu, Z. Zhu, and H. Zhang, "Evolution, limitations, advantages, and future challenges of magnesium alloys as materials for aerospace applications," *J Alloys Compd*, vol. 1008, p. 176707, Dec. 2024, doi: 10.1016/j.jallcom.2024.176707.
- [4]. R. S. *et al.*, "An analysis of polymer material selection and design optimization to improve Structural Integrity in 3D printed aerospace components," *Applied Chemical Engineering*, vol. 7, no. 2, p. 1875, Mar. 2024, doi: 10.59429/ace.v7i2.1875.
- [5]. Jobanpreet Singh, K. Srivastawa, S. Jana, C. Dixit, and R. S., "Advancements in Lightweight Materials for Aerospace Structures: A Comprehensive Review," *Acceleron Aerospace Journal*, vol. 2, no. 3, pp. 173–183, Mar. 2024, doi: 10.61359/11.2106-2409.
- [6]. Y. Li, Y. Xiao, L. Yu, K. Ji, and D. Li, "A review on the tooling technologies for composites manufacturing of aerospace structures: materials, structures and processes," *Compos Part A Appl Sci Manuf*, vol. 154, p. 106762, Mar. 2022, doi: 10.1016/j.compositesa.2021.106762.
- [7]. A. Nevcanoglu, B. Aydemir, and H. Ö. Gülsoy, "The Effect of Aging Heat Treatments on Room and High-Temperature Wear Performance of the Inconel 718<sup>TM</sup> Manufactured by Laser Powder Bed Fusion," *Arab J Sci Eng*, Aug. 2024, doi: 10.1007/s13369-024-09523-3.
- [8]. [8] D. A. Shifler, "Structural Alloys in Marine Service," in *LaQue's Handbook of Marine Corrosion*, Wiley, 2022, pp. 453–526. doi: 10.1002/9781119788867.ch18.
- [9]. M. S. Mehranpour, H. Shahmir, A. Derakhshandeh, and M. Nili-Ahmadabadi, "Significance of Ti addition on precipitation in CoCrFeNiMn high-entropy alloy," *J Alloys Compd*, vol. 888, p. 161530, Dec. 2021, doi: 10.1016/j.jallcom.2021.161530.
- [10]. F. Haftlang, A. Zargaran, J. Moon, S. Y. Ahn, J. B. Seol, and H. S. Kim, "Hetero-deformation induced strengthening, precipitation hardening, and metastability engineering in a novel maraging Fe68Ni10Mn10Co10Ti1.5Si0.5 medium entropy alloy," *J Alloys Compd*, vol. 968, p. 171870, Dec. 2023, doi: 10.1016/j.jallcom.2023.171870.
- [11]. R. Xu, M. Li, and Y. Zhao, "A review of microstructure control and mechanical performance optimization of  $\gamma$ -TiAl alloys," *J Alloys Compd*, vol. 932, p. 167611, Jan. 2023, doi: 10.1016/j.jallcom.2022.167611.
- [12]. P. Sathiyamoorthi and H. S. Kim, "High-entropy alloys with heterogeneous microstructure: Processing and mechanical properties," *Prog Mater Sci*, vol. 123, p. 100709, Jan. 2022, doi: 10.1016/j.pmatsci.2020.100709.
- [13]. H. Zhang, N. Yan, H. Liang, and Y. Liu, "Phase transformation and microstructure control of Ti2AlNb-based alloys: A review," *J Mater Sci Technol*, vol. 80, pp. 203–216, Jul. 2021, doi: 10.1016/j.jmst.2020.11.022.
- [14]. G. Lazorenko, A. Kasprzhitskii, and T. Nazdracheva, "Anti-corrosion coatings for protection of steel railway structures exposed to atmospheric environments: A review," *Constr Build Mater*, vol. 288, p. 123115, Jun. 2021, doi: 10.1016/j.conbuildmat.2021.123115.
- [15]. K. Li, Z. Zhu, B. Xiao, J.-L. Luo, and N. Zhang, "State of the art overview material degradation in high-temperature supercritical CO2 environments," *Prog Mater Sci*, vol. 136, p. 101107, Jul. 2023, doi: 10.1016/j.pmatsci.2023.101107.
- [16]. Z. Qu and X. Tian, "Research Progress in the Corrosion Mechanisms and Anticorrosion Technologies of Waste-to-Energy Plant Boilers," *Coatings*, vol. 14, no. 11, p. 1391, Nov. 2024, doi: 10.3390/coatings14111391.
- [17]. T. Sonar, M. Ivanov, E. Trofimov, A. Tingaev, and I. Suleymanova, "An overview of microstructure, mechanical properties and processing of high entropy alloys and its future perspectives in aeroengine applications," *Mater Sci Energy Technol*, vol. 7, pp. 35–60, 2024, doi: 10.1016/j.mset.2023.07.004.
- [18]. M. Karthik, J. Abhinav, and K. V. Shankar, "Morphological and Mechanical Behaviour of Cu–Sn Alloys—A review," *Metals and Materials International*, vol. 27, no. 7, pp. 1915–1946, Jul. 2021, doi: 10.1007/s12540-020-00899-z.
- [19]. S. Septianissa and A. Z. Chandrasari, "Behavior of Bare, Cr3C2-20NiCr, and NiCrAlY coated Fe-Ni Based Superalloy Under Hot Corrosion in a 75 wt.% Na2SO4 + 25wt.% NaCl film at 9000C," *International Journal of Science and Society*, vol. 6, no. 2, pp. 507–517, May 2024, doi: 10.54783/ijisoc.v6i2.1170.

- [20]. S. Septianissa and A. Z. Chandrasari, "Corrosion Rate of ASTM A53 Steel in Seawater Influenced by Variation in Concentration of Mangifera Indica L. Peel Extract," *Journal of Applied Engineering and Technological Science (JAETS)*, vol. 6, no. 1, pp. 550–560, Dec. 2024, doi: 10.37385/jaets.v6i1.5182.
- [21]. M. Laleh *et al.*, "Heat treatment for metal additive manufacturing," *Prog Mater Sci*, vol. 133, p. 101051, Mar. 2023, doi: 10.1016/j.pmatsci.2022.101051.
- [22]. N. Rojas-Arias, F. G. Coury, K. Vanmeensel, S. T. Amancio-Filho, and P. Gargarella, "Heat treating additive-manufactured alloys: A comprehensive review," *J Alloys Compd*, vol. 1005, p. 176035, Nov. 2024, doi: 10.1016/j.jallcom.2024.176035.
- [23]. I. Brodova *et al.*, "Effect of Grain Size on the Properties of Aluminum Matrix Composites with Graphene," *Metals (Basel)*, vol. 12, no. 6, p. 1054, Jun. 2022, doi: 10.3390/met12061054.
- [24]. I. Brodova *et al.*, "Effect of Grain Size on the Properties of Aluminum Matrix Composites with Graphene," *Metals (Basel)*, vol. 12, no. 6, p. 1054, Jun. 2022, doi: 10.3390/met12061054.
- [25]. F. Long *et al.*, "An internal-oxidation-based strategy induced high-density alumina in-situ nanoprecipitation and carbon nanotube interface optimization for co-reinforcing copper matrix composites," *Compos B Eng*, vol. 229, p. 109455, Jan. 2022, doi: 10.1016/j.compositesb.2021.109455.
- [26]. S. Septianissa, K. W. Widantha, and M. Walidi, "INVESTIGATION OF TEMPERATURES AND HOLDING TIMES ON HIGH-STRENGTH LOW-ALLOY STEEL FOR TANK TRACK LINKS," *LOGIC: Jurnal Rancang Bangun dan Teknologi*, vol. 24, no. 2, pp. 87–92, Jul. 2024, doi: 10.31940/logic.v24i2.87-92.
- [27]. S. Septianissa, F. Rohendi, M. Walidi, and Martoni, "Analysis of the Impact of Cooling Medium Temperature on Heat Treatment Properties of AISI 1040 Steel," 2024, pp. 17–26. doi: 10.2991/978-94-6463-618-5\_3.
- [28]. S. Septianissa, B. Prawara, E. A. Basuki, E. Martides, and E. Riyanto, "Improving the hot corrosion resistance of  $\gamma/\gamma'$  in Fe-Ni superalloy coated with Cr<sub>3</sub>C<sub>2</sub>-20NiCr and NiCrAlY using HVOF thermal spray coating," *Int J Electrochem Sci*, vol. 17, no. 12, p. 221231, Dec. 2022, doi: 10.20964/2022.12.27.
- [29]. J. Lauzuardy *et al.*, "MICROSTRUCTURE CHARACTERISTICS OF Cr<sub>3</sub>C<sub>2</sub>-NiCr COATINGS DEPOSITED WITH THE HIGH-VELOCITY OXY-FUEL THERMAL-SPRAY TECHNIQUE," *Materiali in tehnologije*, vol. 58, no. 2, Apr. 2024, doi: 10.17222/mit.2023.869.
- [30]. S. Septianissa and N. N. Suryaman, *Proses Manufaktur*. Bandung: Media Sains Indonesia, 2025. Accessed: Feb. 11, 2025. [Online]. Available: <https://store.medsan.co.id/detail/978-623-512-362-2-proses-manufaktur>
- [31]. S. Septianissa, *Inovasi dalam Ketahanan Korosi Fe-Ni Superalloy: Solusi Pelapisan dan Material*. Media Sains Indonesia, 2025. Accessed: Feb. 11, 2025. [Online]. Available: <https://store.medsan.co.id/detail/978-623-512-358-5-inovasi-dalam-ketahanan-korosi-feni-superalloy-solusi-pelapisan-dan-material>
- [32]. S. Septianissa, "Evaluasi Dampak Proses Retrogression dan Reaging dalam Meningkatkan Ketahanan Korosi pada Material AL7175," *Jurnal Rekayasa Energi dan Mekanika*, vol. 4, no. 2, p. 137, Feb. 2025, doi: 10.26760/JREM.v4i2.137.
- [33]. Selly Septianissa, Wanidya Ni'immallaili Hadining, and Ayu Zahra Chandrasari, "Mechanical and microstructural effects of varying welding currents in GTAW of 7075-T62 aluminum," *Jurnal Polimesin*, vol. 23, no. 1, pp. 32–37, 2025.